Physics Letters B 810 (2020) 135812

Contents lists available at ScienceDirect

Physics Letters B

www.elsevier.com/locate/physletb

Rapidly rotating Δ-resonance-admixed hypernuclear compact stars

Jia Jie Li [a,b,c,*], Armen Sedrakian [d,e], Fridolin Weber [f,g]

[a] School of Physical Science and Technology, Southwest University, Chongqing 400700, China
[b] Institute of Modern Physics, Chinese Academy of Sciences, Lanzhou 730000, China
[c] Institute for Theoretical Physics, J. W. Goethe University, D-60438 Frankfurt am Main, Germany
[d] Frankfurt Institute for Advanced Studies, D-60438 Frankfurt am Main, Germany
[e] Institute of Theoretical Physics, University of Wroclaw, 50-204 Wroclaw, Poland
[f] Department of Physics, San Diego State University, 5500 Campanile Drive, San Diego, CA 92182, USA
[g] Center for Astrophysics and Space Sciences, University of California at San Diego, La Jolla, CA 92093, USA

ARTICLE INFO

Article history:
Received 24 August 2020
Received in revised form 9 September 2020
Accepted 24 September 2020
Available online 30 September 2020
Editor: W. Haxton

Keywords:
Equation of state
Heavy baryons
Compact stars
Rapid rotation
Gravitational waves

ABSTRACT

We use a set of hadronic equations of state derived from covariant density functional theory to study the impact of their high-density behavior on the properties of rapidly rotating Δ-resonance-admixed hyperonic compact stars. In particular, we explore systematically the effects of variations of the bulk energy isoscalar skewness, $Q_{\rm sat}$, and the symmetry energy slope, $L_{\rm sym}$, on the masses of rapidly rotating compact stars. With models for equation of state satisfying all the modern astrophysical constraints, excessively large gravitational masses of around $2.5\,M_\odot$ are only obtained under three conditions: (a) strongly attractive Δ-resonance potential in nuclear matter, (b) maximally fast (Keplerian) rotation, and (c) parameter ranges $Q_{\rm sat} \gtrsim 500$ MeV and $L_{\rm sym} \lesssim 50$ MeV. These values of $Q_{\rm sat}$ and $L_{\rm sym}$ have a rather small overlap with a large sample (total of about 260) parametrizations of covariant nucleonic density functionals. The extreme nature of requirements (a)-(c) reinforces the theoretical expectation that the secondary object involved in the GW190814 event is likely to be a low-mass black hole rather than a supramassive neutron star.

1. Introduction

In recent years there has been a surge of experimental information on the integral parameters of neutron stars, mostly in the form of constraints coming from their observations in gravitational and electromagnetic waves. Among these is the first detection of gravitational waves from the binary neutron star inspiral event GW170817 by the LIGO–Virgo Collaboration which constrained the tidal deformability of a canonical $1.4\,M_\odot$ mass neutron star and thus the equation of state (EoS) of dense matter at a few times nuclear saturation density [1–3]. These upper bounds suggest that the EoS of stellar matter at such (intermediate) densities is medium-soft [4,5].

A direct astrophysical lower bound of $2.14^{+0.10}_{-0.09}\,M_\odot$ (68.3% credibility interval) on the maximum mass of a neutron star was recently obtained from the measurement of the millisecond pulsar PSR J0740+6620 [6]. The analysis of the GW170817 event was used to derive an approximate upper limit on the maximum mass. By combining gravitational waves and electromagnetic signals with numerical relativity simulations, the maximum mass was found to be in the range of 2.15 to $2.30\,M_\odot$ [7–9]. The quasi-universal relations that describe neutron stars and models of kilonovae were used to draw a similar bound on the maximum mass [10]. Combining the lower and upper bounds quoted above, it follows that the maximum mass of a neutron star is in the 2.1-2.3 $M_\odot$ range.

Furthermore, estimates of the mass and radius of the isolated 205.53 Hz millisecond pulsar PSR J0030+0451 were reported from the analysis of the NICER data of the thermal X-ray waveform from this object in 2019 [11,12]. The predicted radius and mass ranges of $R = 13.02^{+1.24}_{-1.06}$ km and $M = 1.44^{+0.15}_{-0.14}\,M_\odot$ (68.3% credibility interval) [12] and the similar results by Ref. [11], exclude both ultra-soft as well as ultra-stiff behavior of the EoS at intermediate densities. In particular, the relativistic (covariant) density functional based models, which predict somewhat larger radii appear to be consistent with the data if the effects of heavy baryons such as hyperons and/or Δ-resonances are taken into account [13–33].

Very recently the LIGO–Virgo Collaboration observed gravitational waves from a compact binary coalescence with an extremely asymmetric mass ratio of involved compact object: the primary

* Corresponding author.
E-mail addresses: jiajieli@itp.uni-frankfurt.de (J.J. Li), sedrakian@fias.uni-frankfurt.de (A. Sedrakian), fweber@sdsu.edu, fweber@ucsd.edu (F. Weber).

https://doi.org/10.1016/j.physletb.2020.135812

black hole mass is 22.2-24.3 $M_\odot$ whereas the secondary mass is 2.50-2.67 $M_\odot$ [34]. The mass of the latter object falls into the so-called "mass-gap" $2.5\,M_\odot \lesssim M \lesssim 5\,M_\odot$ where no compact object had ever been observed before. The absence of electromagnetic counterpart and measurable tidal effects has left the nature of this compact object open to interpretation. In particular, the interesting question arises as to whether the light companion is the most massive neutron star or the lightest black hole discovered to date. Several authors have addressed this issue suggesting that we are dealing with an extremely rapidly rotating nucleonic compact star [35–38]. Rapid rotation is a critical prerequisite of these scenarios, as it allows to increase a neutron star's mass by around $\sim 20\%$ [39–41]. It was also found that static (i.e., non-rotating) nucleonic EoS models can indeed generate massive stars with mass $M \gtrsim 2.5\,M_\odot$, but some of them are not compatible with constraints obtained from GW170817 [42,43]. A connection of the light companion in the GW190814 event with hyperonization in dense matter was addressed by us in Ref. [44] using the well-calibrated DD-ME2 functional and its extension to the hypernuclear sector. As pointed out in this paper, the compact star interpretation of the light companion in GW190814 is in tension with hypernuclear stellar models even in the case of maximal Keplerian rotation. In the present work, we extend this study two-fold. First, we consider in detail the Δ-resonance admixture to the baryonic octet and study the sensitivity of the results on the Δ-potential in nuclear matter within the set-up of our previous work [29]. Secondly, we study the sensitivity of the results with respect to variations of the (not well-constrained) high-density behavior of the nucleonic density functional. To do so we use the well-known Taylor expansions of the bulk and symmetry energies (see for example [45,46]) given by

$$E(\chi,\delta) \simeq E_{\rm sat} + \frac{1}{2!}K_{\rm sat}\chi^2 + \frac{1}{3!}Q_{\rm sat}\chi^3 + E_{\rm sym}\delta^2 + L_{\rm sym}\delta^2\chi + \mathcal{O}(\chi^4, \chi^2\delta^2), \quad (1)$$

where $\chi = (\rho - \rho_{\rm sat})/3\rho_{\rm sat}$, $\delta = (\rho_n - \rho_p)/\rho$, $\rho_{n/p}$ are the neutron/proton densities, and $\rho_{\rm sat}$ is the nuclear saturation density. The first line in the expansion (1) contains the characteristic terms of the isoscalar channel, which are the saturation energy $E_{\rm sat}$, incompressibility $K_{\rm sat}$, and skewness $Q_{\rm sat}$. The second line contains the characteristic quantities of the isovector channel, namely the symmetry energy $E_{\rm sym}$ and its slope parameter $L_{\rm sym}$. Our focus here will be on the "higher-order terms" $Q_{\rm sat}$ and $L_{\rm sym}$ as these are not well-determined so far.

Earlier, in Ref. [36] the authors considered such an expansion in the context of GW190814 being a fast-spinning neutron star, but without an explicit reference to the particle content of the underlying model. Indeed, expansions like (1) can predict only the amount of isospin in the matter, but are agnostic to its particle content (unless one assumes that only neutrons and protons are present). Even less informative on the particle content are the models which employ constant speed-of-sound EoS [47–49] or piece-wise polytropic EoS [38,50], and such approaches cannot be applied to study hypernuclear and/or Δ-admixed matter. To gain an access to the particle content of the star, we map the EoS given by the expansion (1) for each set of parameters $Q_{\rm sat}$ and $L_{\rm sym}$ to a nucleonic density functional, then we take into account hyperons and Δ-resonances with the parameters tuned to the most plausible hyperon/resonance potentials extracted from nuclear data.

In closing, we mention that an interesting physical possibility of the behavior of superdense matter, which is not being studied here, concerns the transition from hadronic to deconfined quark matter; for recent discussions of this topic, see Refs. [32,49,51–55]. This possibility in the present context of GW190814 event was discussed in Refs. [56,57].

The paper is organized as follows. In Sec. 2 we briefly review the key features of the covariant density functional (CDF) model for hadronic matter. Particular attention is paid to the expansion coefficients $Q_{\rm sat}$ and $L_{\rm sym}$ for nucleonic matter. This is followed in Sec. 3 by a discussion of the bulk properties (in particular maximal possible masses) of compact star models computed for a broad collection of EoS identified in terms of $Q_{\rm sat}$ and $L_{\rm sym}$. The key findings of our study and their implications for the interpretation of the GW190814 event are summarized in Sec. 4.

2. CDF model for hadronic matter

At supranuclear density, hyperonization becomes a serious possibility since hyperons are energetically favored in the cores of neutron stars [58,59]. The presence of hyperons entails a considerable softening of the EoS which lowers the (maximum) masses of neutron stars. In particular, such stars have maximum masses that are smaller than those of neutron stars based on purely nucleonic EoS [14–18,29,30,60–62]. At present, the existence of new degrees of freedom in the cores of neutron stars can neither be confirmed nor ruled out based on astrophysical observations alone. Indeed, one can readily generate hypernuclear EoS supporting a $2\,M_\odot$ compact star [14–18,20,29,30,61,62]. In particular, CDF-based models are versatile enough to generate hypernuclear EoS supporting a $2\,M_\odot$ compact star by fitting the parameters of the interactions in the hyperonic sector to hypernuclear data [17,22,61,62]. These models, however, predict relatively large radii and tidal deformabilities for neutron stars with canonical masses of around $1.4\,M_\odot$, which is disfavored by the GW170817 data [30,63]. This issue can be resolved if excited baryon states, in particular the Δ-resonance, are taken into account in the treatment of β-equilibrated compact star matter [24,29,31]. As shown in Refs. [30,31,63], including the Δ-resonance in hypernuclear CDF calculations leads to neutron star masses and radii that are no longer at variance with the values inferred for those quantities from the observations of GW170817.

Here, we use the standard form of the CDF in which Dirac baryons are coupled to mesons with density-dependent couplings [64,65]. The theory is Lorentz invariant and, therefore, preserves causality when applied to high-density matter. The baryons interact via the exchanges of σ, ω, and ρ mesons, which comprise the minimal set of mesons necessary for a quantitative description of nuclear phenomena. In addition, we consider two hidden-strangeness mesons (σ^*, ϕ) which describe interactions between hyperons.

The Lagrangian of the theory is given by the sum of the free baryonic and mesonic Lagrangians, which can be found in Refs. [18,62,66], and the interaction Lagrangian which reads

$$\mathscr{L}_{\rm int} = \sum_B \bar\psi_B \Big(- g_{\sigma B}\sigma - g_{\sigma^* B}\sigma^* - g_{\omega B}\gamma^\mu\omega_\mu - g_{\phi B}\gamma^\mu\phi_\mu - g_{\rho B}\gamma^\mu\vec\rho_\mu\cdot\vec\tau_B\Big)\psi_B + \sum_D(\psi_B \to \psi^\nu_D), \quad (2)$$

where ψ stands for the Dirac spinors and ψ^ν for the Rarita-Schwinger spinors [67]. Index B labels the particles of the spin-1/2 baryonic octet, which comprises nucleons $N \in \{n, p\}$ and hyperons $Y \in \{\Lambda, \Xi^{0,-}, \Sigma^{+,0,-}\}$, while index D refers to the spin-3/2 resonance quartet of Δ's (i.e., $\Delta \in \{\Delta^{++,+,0,-}\}$). The mesons couple to the baryonic octet and the Δ's with the strengths determined by the coupling constants g_{mB} and g_{mD}, which are functions of the baryonic density, $g_{mB(D)}(\rho) = g_{mB(D)}(\rho_{\rm sat})f_m(r)$, where $r = \rho/\rho_{\rm sat}$. There are in total four free parameters (three in isoscalar sector and one in isovector sector) for functions $f_m(r)$, which allow one to adjust the characteristic terms for nucleonic matter $K_{\rm sat}$, $Q_{\rm sat}$,

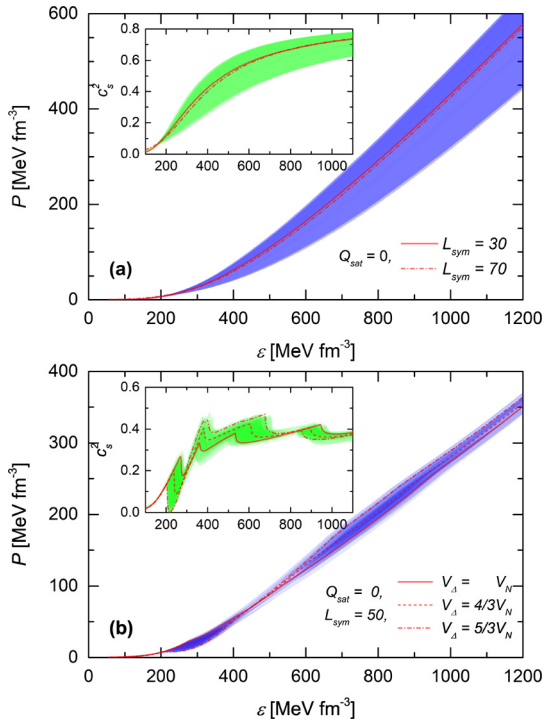

Fig. 1. EoS and the corresponding speed-of-sound squared for (a) purely nucleonic and (b) Δ-hyperon admixed stellar matter. In (a) the nucleonic EoS models are generated by varying the parameters $Q_{\rm sat} \in [-600, 900]$ MeV and $L_{\rm sym} \in [30, 70]$ MeV. The EoS with $Q_{\rm sat} = 0$, $L_{\rm sym} = 30$ and 70 MeV are shown by solid and dash-dotted lines for illustration. In (b) Δ-admixed hyperonic matter EoS are generated by varying the parameters $Q_{\rm sat} \in [300, 900]$ MeV, $L_{\rm sym} \in [30, 70]$ MeV for values of Δ-potential V_D in isospin symmetric nuclear matter $V_D/V_N = 1, 4/3$ and $5/3$, where V_N is the nucleonic potential. The EoS models with $Q_{\rm sat} = 600$, $L_{\rm sym} = 50$ MeV and three indicated values of V_D are shown for illustration.

$L_{\rm sym}$ in expansion (1) and $\rho_{\rm sat}$, see Ref. [63] for detailed discussion of the flexibility of functions $f_m(r)$. This study also suggests that one can generate a set of nucleonic CDF models by varying only $Q_{\rm sat}$ or $L_{\rm sym}$ while keeping the lower-order parameters fixed.

The Lagrangian (2) is minimal, as it does not contain (a) the isovector-scalar δ meson [68] and (b) the π meson and the tensor couplings of vector mesons to baryons (both of which arise in the Hartree-Fock theory [62]). As shown below in Sec. 3, a wide range of the mass-radius relations can be generated by this Lagrangian which covers parameter space comparable with the recent meta-modeling for realistic nucleonic EoS [43]. We note also that other spin-3/2 resonances (like Σ^{-*} which has a slightly heavier mass than Δ) may also appear in dense matter. However, their potentials in nuclear matter are unknown. We thus consider only the lightest (non-strange) members of the baryon $J^{3/2}$-decouplet.

For our analysis below we adopt, as a reference, the DD-ME2 parametrization [66] which was calibrated to the properties of finite nuclei. This parametrization has been tested on the entire nuclear chart with great success and agrees with experimentally known bounds on the empirical parameters of nuclear matter. In the hypernuclear sector, the vector meson-hyperon couplings are given by the SU(6) spin-flavor-symmetric quark model, whereas the scalar meson-hyperon couplings are determined by fitting them to the potentials extracted from hypernuclear systems. For the resonance sector, the vector meson-Δ couplings are chosen close to the meson-N ones, whereas the scalar meson-Δ couplings are determined by fitting them to certain preselected potentials extracted from heavy-ion collisions and the scattering of electrons and pions off nuclei (for an overview see Refs. [24,28,29,33]). Note that in this manner *we assume that the hyperon and Δ potentials scale with density the same way as the nucleonic potentials, and therefore their high-density behavior is inferred from that of the nucleons.* This assumption has its justification in the quark substructure of the constituents. However, first-principle computations that may support our assumption is still lacking. See Refs. [30,63] for details of the model.

The nuclear matter EoS can be characterized in terms of the double expansion, shown in Eq. (1), around the saturation density and the isospin symmetrical limit. In Refs. [45,63] it has been shown that the gross properties of compact stars are very sensitive to the higher-order empirical parameters of nuclear matter around the saturation density, specifically to the isoscalar skewness $Q_{\rm sat}$ and isovector slope $L_{\rm sym}$. Note also that the low-order empirical parameters are well constrained by physics of finite nuclei. The combined analysis of terrestrial experiments and astrophysical observations predict a value for the slope of symmetry energy $L_{\rm sym} = 58.7 \pm 28.1$ MeV [69]. The skewness $Q_{\rm sat}$ is highly model dependent. For example, non-relativistic Skyrme or Gogny models predict (predominantly) negative $Q_{\rm sat}$ value [45,70], whereas relativistic models predict both positive and negative $Q_{\rm sat}$ values [45,71,72]. With this in mind, we vary $Q_{\rm sat}$ and/or $L_{\rm sym}$ individually within a wide range and study their impact on the properties of compact stars, by modifying (only!) the density-dependence of the functional at high density; its well-tuned features at and around the saturation density remain fixed as the defaults of DD-ME2 [66], namely, $K_{\rm sat} = 251.2$ MeV and $E_{\rm sym} = 32.3$ MeV.

Fig. 1 shows the EoS and the corresponding speed-of-sound squared for purely nucleonic and Δ-admixed hyperonic stellar matter for a range of the parameters $Q_{\rm sat}, L_{\rm sym}$ and values of Δ-potential V_D in symmetric nuclear matter ($V_D/V_N = 1, 4/3$ and $5/3$, where V_N is the nucleonic potential). All those EoS models fulfill the constraints of $2\,M_\odot$ observations [6,73]. The results for Δ-admixed hyperonic stellar matter with $V_D/V_N < 1$ are not shown, since in this case, the Δ population is rather small [29,31]. In Fig. 1(b) we illustrate also the EoSs of Δ-admixed hyperonic matter for three values of Δ-potential. It is seen that Δ's *soften* the EoS at low densities which directly implies smaller radii for not very massive members of the sequences. This effect increases with the depth of the Δ-potential, i.e., the larger is the attractive the Δ-potential, the smaller is the radius of the intermediate-mass compact star (see Fig. 4 below).

3. Results and discussions

3.1. Nucleonic EoS models

We first consider static (non-rotating) as well as rapidly rotating compact stars made of purely nucleonic matter. Figs. 2(a) and (b) show the mass-radius and mass-tidal deformability relationships computed for $Q_{\rm sat}$ values -600, -300, 0, 300, 600, and 900 MeV (in that order from left to right) and $L_{\rm sym}$ values of 30 (red curves), 50 (green curves), and 70 MeV (blue curves). Observational constraints from multi-messenger astronomy are highlighted. These concern the masses of PSR J0348+0432 [73] and PSR J0740+6620 [6], the compactness and tidal deformability constraints extracted from the binary compact star mergers GW170817 [5,74,75] and GW190425 [76], the mass and radius measurements for PSR J0030+0451 by NICER [11,12], and the mass of the secondary component of GW190814 [34].

One sees from Fig. 2(a) that compact stars with masses of around $M \sim 2.5\,M_\odot$ require nucleonic EoS models with large and positive $Q_{\rm sat}$ values in the range $Q_{\rm sat} \gtrsim 600$ MeV, where $L_{\rm sym}$ can be 30, 50, or 70 MeV. These EoS models, however, lead to $12.9 \lesssim R_{1.4} \lesssim 13.7$ km for the radius of a $1.4\,M_\odot$ star, as can be read off from Fig. 2(a), and to tidal deformabilities $\Lambda_{1.4} \gtrsim 700$ (Fig. 2(b)), both of which being at variance with GW170817 observation [5]. In fact the revised upper limit on $\Lambda_{1.4}$ is 190^{+390}_{-120} (90%

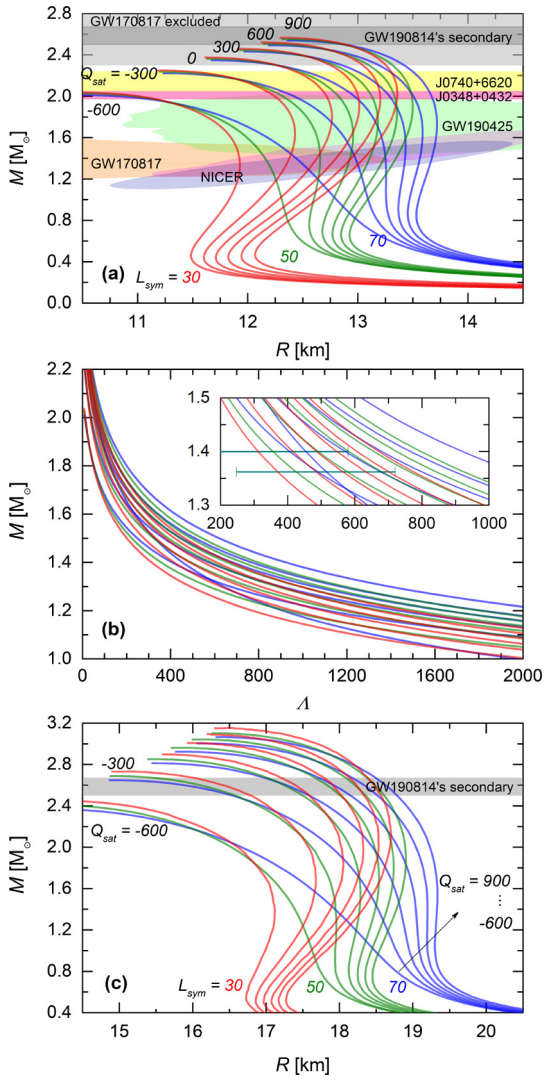

Fig. 2. Mass-radius (a) and mass-tidal deformability (b) relations of static (i.e., non-rotating), purely nucleonic stellar configurations generated by tuning the isoscalar skewness coefficient $Q_{\rm sat}$ and the slope of symmetry energy $L_{\rm sym}$. Modern constraints from multi-messenger astronomy are shown by the color regions (see text for details). (c) Same as (a), but for rapidly rotating (Keplerian) sequences.

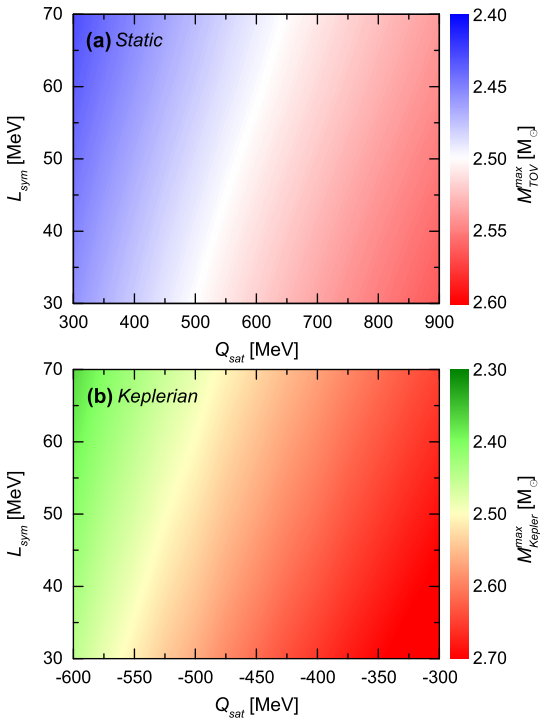

Fig. 3. The maximum masses of (a) static and (b) Keplerian purely nucleonic stellar sequences (color coded column on the right) for a range of values spanned by $Q_{\rm sat}$ and $L_{\rm sym}$. The large-$Q_{\rm sat}$ and small-$L_{\rm sym}$ range corresponds to compact stars with masses exceeding 2.5 $M_\odot$.

credibility interval) [5], which does not overlap with $\Lambda_{1.4} \gtrsim 700$. Furthermore, we checked that the EoSs for symmetric nuclear matter computed with these models are much stiffer than the range of admissible EoS deduced from studies of heavy-ion collisions [77]. A similar conclusion was reached also in a recent work where the nonlinear CDF models were used [42].

The only EoS models that lead to $\Lambda_{1.4}$ values compatible with $\Lambda_{1.4} = 190^{+390}_{-120}$ are those computed for ($L_{\rm sym} = 30$ MeV, $Q_{\rm sat} \lesssim 300$ MeV), ($L_{\rm sym} = 50$ MeV, $Q_{\rm sat} \lesssim 0$ MeV) and ($L_{\rm sym} = 70$, MeV, $Q_{\rm sat} \lesssim -300$ MeV), as can be deduced from the curves shown in the inset in Fig. 2(b). All these combinations correspond to $\Lambda_{1.4} \lesssim 580$ MeV, the upper bound of inferred $\Lambda_{1.4} = 190^{+390}_{-120}$. In summary, we conclude that the low tidal deformability of a 1.4 $M_\odot$ compact star inferred from GW170817 makes it highly unlikely that the maximum mass of a static, nucleonic neutron star could be as high as $\sim 2.5\,M_\odot$.

Next, we turn to the maximally rotating stellar models shown in Fig. 2(c). There exist several codes for computing configurations of rapidly rotating compact stars, all of which are based on the iterative method of solution of Einstein's equations [40,78] in axial symmetry for any tabulated EoS. The method starts with a "guess" density profile, integrates the stellar structure equations, thus obtaining a new input density profile for the following iteration. This procedure is repeated until convergence is achieved at each point of the spatial grid. In our computations, we use the public domain RNS code[1] which implements this scheme. Each star shown in this figure rotates at its respective (general relativistic) Kepler frequency, at which mass shedding from the equator terminates stable rotation. There are other rotational instabilities (like the r-modes) which set a tighter limit on stable rotation than the Kepler frequency does. However, the Kepler frequency is particularly interesting as it sets an absolute limit on rapid rotation, and it also enables stars to carry the maximum amount of mass. From model calculation it is known that the gravitational mass increase can be as large as around 20% [39,40] compared to non-rotating stars. As shown in Fig. 2(c), almost all EoS models are capable of producing a compact star whose mass falls in the mass range estimated for the secondary in GW190814. The only models that fail are those based on very negative $Q_{\rm sat}$ values (e.g., $Q_{\rm sat} = -600$ MeV), independent of the value chosen for $L_{\rm sym}$. The $Q_{\rm sat} = -300$ MeV EoS models, which fail to support a non-rotating $\sim 2.5\,M_\odot$ compact star (Fig. 2(a)), now support stars with masses exceeding 2.6 $M_\odot$.

The dependence of the maximum masses for static and Keplerian models on the relevant range of $Q_{\rm sat}$ and $L_{\rm sym}$ parameters for purely nucleonic EoS models is shown in Fig. 3. It allows one to easily read-off the maximum masses predicted by any density functional once its values for $Q_{\rm sat}$ and $L_{\rm sym}$ are known.

To summarize, (i) static nucleonic compact stars with masses up to 2.5 $M_\odot$ can be obtained for $Q_{\rm sat} \gtrsim 600$ MeV, however, the tidal deformability $\Lambda_{1.4}$ for such models is in tension with the inference from GW170817; (ii) this tension is lifted if one assumes that the unknown secondary in GW190814 is a rapidly rotating neutron star composed of nucleonic matter [35–37]; (iii) neverthe-

[1] www.gravity.phys.uwm.edu/rns/.

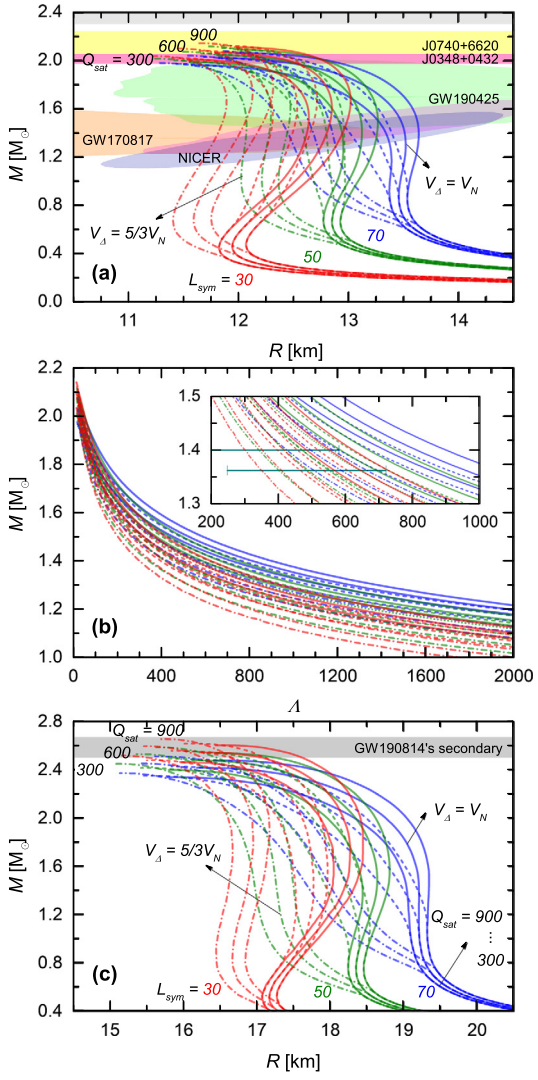

Fig. 4. Mass-radius (a) and mass-tidal deformability (b) relations of static stellar configurations containing hyperon-Δ-admixed matter, generated by tuning the isoscalar skewness coefficient $Q_{\rm sat}$ and the slope of symmetry energy $L_{\rm sym}$, and the Δ-potential at nuclear saturation density $V_\Delta/V_N = 1$ (solid lines), 4/3 (dashed), and 5/3 (dash-dotted). (c) Same as (a), but for rapidly rotating (Keplerian) sequences.

less, if $Q_{\rm sat} \leq -500$ MeV, the static (Tolman-Oppenheimer-Volkoff) maximum masses of the models are $M_{\rm TOV}^{\rm max} \leq 2.1\,M_\odot$ and such models are in agreement with tidal deformability values $\Lambda_{1.4}$ derived from the GW170817 event and the radius values $R_{1.4}$ obtained from NICER's X-ray observations [11,12]. In this case the secondary of GW190814 must be a black hole.

3.2. Hyperon-Δ admixed EoS models

Since the matter in the cores of compact stars is compressed to densities several times higher than the density of atomic nuclei, the core composition may contain substantial populations of hyperons and, as emphasized in several recent papers, by Δ's too [24–31,79,80]. The possible presence of Δ's in the cores of neutron stars has not been considered for years since the early CDF calculations did show that the Δ-resonance would appear at densities too high to be reached in the cores of compact stars [58]. However, calculations based on more sophisticated microscopic models and/or tighter constraints on the model parameters [24–31,79–81] show that Δ's could make up a large fraction of the baryon population in neutron star matter and could also have a significant effect on the radii of compact stars [29,31,81].

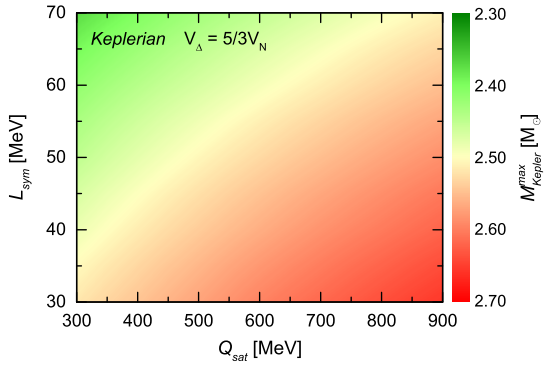

Fig. 5. The maximum masses of Keplerian sequences as a function parameter space spanned by $Q_{\rm sat}$ and $L_{\rm sym}$. The Δ-resonance potential is fixed at the largest value $V_\Delta = 5/3V_N$ considered in this work. The large-$Q_{\rm sat}$ and small-$L_{\rm sym}$ range corresponds to compact stars with masses exceeding $2.5\,M_\odot$.

In Figs. 4(a) and (b) the mass-radius and mass-tidal deformability relations computed for Δ-admixed hyperonic EoS models are shown for $Q_{\rm sat}$ values ranging from 300 to 900 MeV, $L_{\rm sym}$ values of 30, 50 and 70 MeV, and different values for the Δ-potential V_Δ at nuclear saturation density. As can be seen, to support a compact star with a gravitational mass of about $2\,M_\odot$, containing hyperons and Δ's in its core, $Q_{\rm sat}$ needs to be at least as large as ~ 300 MeV. The maximum possible mass of the static stellar sequence is $M_{\rm TOV}^{\rm max} \simeq 2.2\,M_\odot$.

Imposing the $\Lambda_{1.4} = 190^{+390}_{-120}$ constraint on the EoS, it follows from Fig. 4(b) that all hyperon-Δ-admixed EoS models are consistent with this constraint if the Δ-potential is assumed to be $V_\Delta/V_N = 5/3$, independent of the particular choices of $Q_{\rm sat}$ and $L_{\rm sym}$. The situation is strikingly different for $V_\Delta/V_N = 1$ in which case only $Q_{\rm sat} = 300$ and 600 MeV are allowed for $L_{\rm sym} = 30$ MeV. For $L_{\rm sym} = 70$ MeV none of the three $Q_{\rm sat}$ values leads to tidal deformabilities that are in agreement with $\Lambda_{1.4} \leq 580$.

Fig. 4(c) shows the mass-radius relationships of maximally rotating (Keplerian) stellar models computed for our collection of Δ-admixed hyperonic EoS models. As can be seen, the rotation at the mass shedding limit increases the maximum-possible gravitational mass to values in the range of $2.4\,M_\odot \lesssim M_{\rm Kepler}^{\rm max} \lesssim 2.7\,M_\odot$, depending on the $Q_{\rm sat}$ and $L_{\rm sym}$ values and the depth of the Δ-potential. The largest values for $M_{\rm Kepler}^{\rm max}$ are obtained for $Q_{\rm sat} \geq 600$ MeV, $L_{\rm sym} \leq 50$ MeV, and $V_\Delta/V_N = 5/3$. All these models for the EoS lead to masses that are consistent with the mass estimated for the stellar secondary of the GW170817 event.

The dependence of maximum masses of the Keplerian models on the range of $Q_{\rm sat}$ and $L_{\rm sym}$ parameters in the case $V_\Delta = 5/3V_N$ is shown in Fig. 5. We note that the range of $Q_{\rm sat}$ value extracted from our analysis has a rather small overlap with the ones extracted from large samples of non-relativistic and relativistic density functionals [70,71]. We thus conclude that for the secondary object in GW190814 to be a compact star featuring heavy baryons requires several extreme assumptions, which apart from maximally rapid rotation, requires large values for the Δ-resonance potential in nuclear matter and combinations of $Q_{\rm sat}$ and $L_{\rm sym}$ that fall outside the range covered by all known density functionals, except DD-ME2 [66] and a few newly proposed functionals [42,82]. These findings support the theoretical expectation that the secondary stellar object involved in the GW190814 event is a low-mass black hole rather than a supermassive neutron star.

Finally, it should be mentioned that in this work the vector meson-hyperon couplings are given by the SU(6) spin-flavor symmetric quark model. If one fixes the couplings according to the more general SU(3) flavor symmetry, the maximum mass of static compact stars would increase by about 10% [15,62]. However, we anticipate that modification of vector meson-hyperon cou-

plings will not change our main conclusion about the nature of GW190814's secondary member.

4. Summary and conclusions

In this work, we have investigated properties of non-rotating as well as rapidly rotating compact stars with and without Δ-resonance-admixed hyperonic core compositions. The corresponding models for the EoS are generated with covariant density functional theory. The high-density behavior of nucleonic EoS is quantified in terms of the isoscalar skewness coefficient $Q_{\rm sat}$ and the isovector slope coefficient $L_{\rm sym}$. The hyperon potentials are tuned to the most plausible potentials extracted from hypernuclear data. The Δ-potential in nuclear matter is taken to be in the range $1 \leq V_\Delta/V_N \leq 5/3$, as no consensus has been reached yet on its magnitude. The density-dependences of the hyperon- and Δ-meson couplings are assumed to be the same as those of nucleons.

We found that purely nucleonic models for the EoS can accommodate compact stars as massive as $M \simeq 2.5\,M_\odot$, but only if the isoscalar skewness coefficient $Q_{\rm sat} \gtrsim 600$ MeV. These EoS models, however, lead to tidal deformabilities for a $1.4\,M_\odot$ star that conflict with observation and are thus ruled out as valid EoS models. To resolve the tidal deformability issue, one must have $Q_{\rm sat} \lesssim 300$ MeV. The problem that arises from these EoS models, however, is that they then no longer support a $2.5\,M_\odot$ star and thus qualify either. The maximal possible rotation rate at the mass shedding limit resolves this issue as it pushes the masses of most (with the exception of $Q_{\rm sat} \lesssim -550$ MeV) stellar sequences up to the $\sim 2.5\,M_\odot$ mass range. This confirms the earlier findings [35–37] that a rapidly, uniformly rotating compact star made of purely nucleonic matter could have been the secondary stellar object involved in the GW190814 event.

Taking hyperon and Δ-resonance populations into account our EoS models reduces the masses of compact stars. In particular, the maximal masses of non-rotating stars are reduced to $2.0\,M_\odot \lesssim M \lesssim 2.2\,M_\odot$ if $Q_{\rm sat} \gtrsim 300$ MeV. So none of these models comes even close to the $2.5\,M_\odot$ constraint set by GW190814. This is different if rapid rotation at the mass shedding frequency is considered. In this case, the stellar models computed for a strongly attractive Δ-potential in nuclear matter of $V_\Delta/V_N = 5/3$ reach the $2.5\,M_\odot$ mass limit rather comfortably. The situation is strongly depending on the $Q_{\rm sat}$ and $L_{\rm sym}$ values, as graphically illustrated in Fig. 5. The smallest value for $Q_{\rm sat}$ is $Q_{\rm sat} \approx 300$ MeV for $L_{\rm sym} = 30$ MeV, while $Q_{\rm sat} \approx 900$ MeV for $L_{\rm sym} = 70$ Mev. We note that all the valid EoS models in this figure lead to $R_{1.4}$ and $\Lambda_{1.4}$ values that are in agreement with observation. For EoS models computed with Δ-potential $V_\Delta/V_N = 1$, the agreement is either only marginal or can not be reached at all. The combinations required for $Q_{\rm sat}$ and $L_{\rm sym}$ lie outside the range covered by presently known non-relativistic and relativistic nuclear density functionals. A few exceptions to this are the functionals with values $Q_{\rm sat} \gtrsim 500$ MeV and the possibility of $M^{\rm max}_{\rm Kepler}/M_\odot \gtrsim 2.5$.

To summarize, current valid EoS models which account for Δ-admixed hyperonic matter in the cores of compact stars imply that the secondary object in the GW190814 event was most likely a low-mass black hole, confirming our earlier conclusion [44]. Nevertheless, a neutron star interpretation cannot be excluded at this time, but would require a range of extreme assumptions: (a) rapid (Keplerian) rotation, which may not be reached due to various instabilities that may set in at lower rotation frequencies; (b) strongly attractive Δ-resonance potential in symmetric nuclear matter; (c) large, positive value of the isoscalar skewness $Q_{\rm sat}$ parameter.

Declaration of competing interest

The authors declare that they have no known competing financial interests or personal relationships that could have appeared to influence the work reported in this paper.

Acknowledgements

This work was, in part, supported by European COST Actions "PHAROS" (CA16214). The research of J.J.L. at Goethe University was supported by the Alexander von Humboldt Foundation. A.S. is supported by the Deutsche Forschungsgemeinschaft (Grant No. SE 1836/5-1) and F.W. is supported through the U.S. National Science Foundation under Grants PHY-1714068 and PHY-2012152.

References

[1] B.P. Abbott, R. Abbott, R.X. Adhikari, A. Ananyeva, S.B. Anderson, et al., Multi-messenger observations of a binary neutron star merger, Astrophys. J. Lett. 848 (2017) L12, https://doi.org/10.3847/2041-8213/aa91c9.
[2] B.P. Abbott, R. Abbott, T.D. Abbott, F. Acernese, K. Ackley, et al., Gravitational waves and gamma-rays from a binary neutron star merger: GW170817 and GRB170817A, Astrophys. J. Lett. 848 (2017) L13, https://doi.org/10.3847/2041-8213/aa920c.
[3] B.P. Abbott, R. Abbott, T.D. Abbott, F. Acernese, K. Ackley, et al., GW170817: observation of gravitational waves from a binary neutron star inspiral, Phys. Rev. Lett. 119 (2017), https://doi.org/10.1103/PhysRevLett.119.161101 161101.
[4] B.P. Abbott, R. Abbott, T.D. Abbott, F. Acernese, K. Ackley, et al., GW170817: measurements of neutron star radii and equation of state, Phys. Rev. Lett. 121 (2018) 161101, https://doi.org/10.1103/PhysRevLett.121.161101.
[5] B.P. Abbott, R. Abbott, T.D. Abbott, F. Acernese, K. Ackley, et al., Properties of the binary neutron star merger GW170817, Phys. Rev. X 9 (2019) 011001, https://doi.org/10.1103/PhysRevX.9.011001.
[6] H. Cromartie, E. Fonseca, S.M. Ransom, P.B. Demorest, Z. Arzoumanian, et al., Relativistic Shapiro delay measurements of an extremely massive millisecond pulsar, Nat. Astron. 4 (2020) 72–76, https://doi.org/10.1038/s41550-019-0880-2.
[7] B. Margalit, B.D. Metzger, Constraining the maximum mass of neutron stars from multi-messenger observations of GW170817, Astrophys. J. Lett. 850 (2017) L19, https://doi.org/10.3847/2041-8213/ab2ae2.
[8] M. Shibata, S. Fujibayashi, K. Hotokezaka, K. Kiuchi, K. Kyutoku, et al., Modeling GW170817 based on numerical relativity and its implications, Phys. Rev. D 96 (2017) 123012, https://doi.org/10.1103/PhysRevD.96.123012.
[9] M. Ruiz, S.L. Shapiro, A. Tsokaros, GW170817, general relativistic magnetohydrodynamic simulations, and the neutron star maximum mass, Phys. Rev. D 97 (2018) 021501, https://doi.org/10.1103/PhysRevD.97.021501.
[10] L. Rezzolla, E.R. Most, L.R. Weih, Using gravitational-wave observations and quasi-universal relations to constrain the maximum mass of neutron stars, Astrophys. J. Lett. 852 (2018) L25, https://doi.org/10.3847/2041-8213/aaa401.
[11] T.E. Riley, A.L. Watts, S. Bogdanov, P.S. Ray, R.M. Ludlam, et al., A NICER view of PSR J0030+0451: millisecond pulsar parameter estimation, Astrophys. J. Lett. 887 (2019) L21, https://doi.org/10.3847/2041-8213/ab481c.
[12] M.C. Miller, F.K. Lamb, A.J. Dittmann, S. Bogdanov, Z. Arzoumanian, et al., PSR J0030+0451 mass and radius from NICER data and implications for the properties of neutron star matter, Astrophys. J. Lett. 887 (2019) L24, https://doi.org/10.3847/2041-8213/ab50c5.
[13] L. Bonanno, A. Sedrakian, Composition and stability of hybrid stars with hyperons and quark color-superconductivity, Astron. Astrophys. 539 (2012) A16, https://doi.org/10.1051/0004-6361/201117832.
[14] S. Weissenborn, D. Chatterjee, J. Schaffner-Bielich, Hyperons and massive neutron stars: the role of hyperon potentials, Nucl. Phys. A 881 (2012) 62–77, https://doi.org/10.1016/j.nuclphysa.2012.02.012.
[15] S. Weissenborn, D. Chatterjee, J. Schaffner-Bielich, Hyperons and massive neutron stars: vector repulsion and su(3) symmetry, Phys. Rev. C 85 (2012) 065802, https://doi.org/10.1103/PhysRevC.85.065802.
[16] G. Colucci, A. Sedrakian, Equation of state of hypernuclear matter: impact of hyperon–scalar-meson couplings, Phys. Rev. C 87 (2013) 055806, https://doi.org/10.1103/PhysRevC.87.055806.
[17] E. van Dalen, G. Colucci, A. Sedrakian, Constraining hypernuclear density functional with Λ-hypernuclei and compact stars, Phys. Lett. B 734 (2014) 383–387, https://doi.org/10.1016/j.physletb.2014.06.002.
[18] M. Oertel, C. Providência, F. Gulminelli, A.R. Raduta, Hyperons in neutron star matter within relativistic mean-field models, J. Phys. G, Nucl. Part. Phys. 42 (2015) 075202, https://doi.org/10.1088/0954-3899/42/7/075202.
[19] D. Chatterjee, I. Vidaña, Do hyperons exist in the interior of neutron stars?, Eur. Phys. J. A 52 (2016) 29, https://doi.org/10.1140/epja/i2016-16029-x.

[20] T. Katayama, K. Saito, Hyperons in neutron stars, Phys. Lett. B 747 (2015) 43–47, https://doi.org/10.1016/j.physletb.2015.03.039.
[21] M. Fortin, C. Providência, A.R. Raduta, F. Gulminelli, J.L. Zdunik, et al., Neutron star radii and crusts: uncertainties and unified equations of state, Phys. Rev. C 94 (2016) 035804, https://doi.org/10.1103/PhysRevC.94.035804.
[22] M. Fortin, S.S. Avancini, C. Providência, I. Vidaña, Hypernuclei and massive neutron stars, Phys. Rev. C 95 (2017) 065803, https://doi.org/10.1103/PhysRevC.95.065803.
[23] Y. Chen, H. Guo, Y. Liu, Neutrino scattering rates in neutron star matter with Δ isobars, Phys. Rev. C 75 (2007) 035806, https://doi.org/10.1103/PhysRevC.75.035806.
[24] A. Drago, A. Lavagno, G. Pagliara, D. Pigato, Early appearance of Δ isobars in neutron stars, Phys. Rev. C 90 (2014) 065809, https://doi.org/10.1103/PhysRevC.90.065809.
[25] B.-J. Cai, F.J. Fattoyev, B.-A. Li, W.G. Newton, Critical density and impact of $\Delta(1232)$ resonance formation in neutron stars, Phys. Rev. C 92 (2015) 015802, https://doi.org/10.1103/PhysRevC.92.015802.
[26] Z.-Y. Zhu, A. Li, J.-N. Hu, H. Sagawa, $\Delta(1232)$ effects in density-dependent relativistic Hartree-Fock theory and neutron stars, Phys. Rev. C 94 (2016) 045803, https://doi.org/10.1103/PhysRevC.94.045803.
[27] H.S. Sahoo, G. Mitra, R. Mishra, P.K. Panda, B.-A. Li, Neutron star matter with Δ isobars in a relativistic quark model, Phys. Rev. C 98 (2018) 045801, https://doi.org/10.1103/PhysRevC.98.045801.
[28] E.E. Kolomeitsev, K.A. Maslov, D.N. Voskresensky, Delta isobars in relativistic mean-field models with σ-scaled hadron masses and couplings, Nucl. Phys. A 961 (2017) 106–141, https://doi.org/10.1016/j.nuclphysa.2017.02.004.
[29] J.J. Li, A. Sedrakian, F. Weber, Competition between delta isobars and hyperons and properties of compact stars, Phys. Lett. B 783 (2018) 234–240, https://doi.org/10.1016/j.physletb.2018.06.051.
[30] J.J. Li, A. Sedrakian, Implications from GW170817 for Δ-isobar admixed hypernuclear compact stars, Astrophys. J. Lett. 874 (2019) L22, https://doi.org/10.3847/2041-8213/ab1090.
[31] P. Ribes, A. Ramos, L. Tolos, C. Gonzalez-Boquera, M. Centelles, Interplay between Δ particles and hyperons in neutron stars, Astrophys. J. 883 (2019) 168, https://doi.org/10.3847/1538-4357/ab3a93.
[32] J.J. Li, A. Sedrakian, M. Alford, Relativistic hybrid stars with sequential first-order phase transitions and heavy-baryon envelopes, Phys. Rev. D 101 (2020) 063022, https://doi.org/10.1103/PhysRevD.101.063022.
[33] A.R. Raduta, M. Oertel, A. Sedrakian, Proto-neutron stars with heavy baryons and universal relations, arXiv:2008.00213, 2020.
[34] R. Abbott, T.D. Abbott, S. Abraham, F. Acernese, K. Ackley, et al., GW190814: gravitational waves from the coalescence of a 23 solar mass black hole with a 2.6 solar mass compact object, Astrophys. J. Lett. 896 (2020) L44, https://doi.org/10.3847/2041-8213/ab960f.
[35] E.R. Most, L.J. Papenfort, L.R. Weih, L. Rezzolla, A lower bound on the maximum mass if the secondary in GW190814 was once a rapidly spinning neutron star, arXiv:2006.14601, 2020.
[36] N.-B. Zhang, B.-A. Li, GW190814's secondary component with mass (2.50-2.67)$M_\odot$ as a super-fast pulsar, arXiv:2007.02513, 2020.
[37] A. Tsokaros, M. Ruiz, S.L. Shapiro, GW190814: spin and equation of state of a neutron star companion, arXiv:2007.05526, 2020.
[38] I. Tews, P.T.H. Pang, T. Dietrich, M.W. Coughlin, S. Antier, et al., On the nature of GW190814 and its impact on the understanding of supranuclear matter, arXiv:2007.06057, 2020.
[39] F. Weber, N.K. Glendenning, Application of the improved Hartle method for the construction of general relativistic rotating neutron star models, Astrophys. J. 390 (1992) 541, https://doi.org/10.1086/171304.
[40] G.B. Cook, S.L. Shapiro, S.A. Teukolsky, Rapidly rotating neutron stars in general relativity: realistic equations of state, Astrophys. J. 424 (1994) 823, https://doi.org/10.1086/173934.
[41] V. Paschalidis, N. Stergioulas, Rotating stars in relativity, Living Rev. Relativ. 20 (2017) 7, https://doi.org/10.1007/s41114-017-0008-x.
[42] F. Fattoyev, C. Horowitz, J. Piekarewicz, B. Reed, GW190814: impact of a 2.6 solar mass neutron star on nucleonic equations of state, arXiv:2007.03799, 2020.
[43] J. Margueron, R. Hoffmann Casali, F. Gulminelli, Equation of state for dense nucleonic matter from metamodeling. II. Predictions for neutron star properties, Phys. Rev. C 97 (2018) 025806, https://doi.org/10.1103/PhysRevC.97.025806.
[44] A. Sedrakian, F. Weber, J.J. Li, Confronting GW190814 with hyperonization in dense matter and hypernuclear compact stars, Phys. Rev. D 102 (2020) 041301, https://doi.org/10.1103/PhysRevD.102.041301.
[45] J. Margueron, R. Hoffmann Casali, F. Gulminelli, Equation of state for dense nucleonic matter from metamodeling. I. Foundational aspects, Phys. Rev. C 97 (2018) 025805, https://doi.org/10.1103/PhysRevC.97.025805.
[46] N.-B. Zhang, B.-A. Li, J. Xu, Combined constraints on the equation of state of dense neutron-rich matter from terrestrial nuclear experiments and observations of neutron stars, Astrophys. J. 859 (2018) 90, https://doi.org/10.3847/1538-4357/aac027.
[47] M.G. Alford, S. Han, M. Prakash, Generic conditions for stable hybrid stars, Phys. Rev. D 88 (2013) 083013, https://doi.org/10.1103/PhysRevD.88.083013.
[48] J.L. Zdunik, P. Haensel, Maximum mass of neutron stars and strange neutron-star cores, Astron. Astrophys. 551 (2013) A61, https://doi.org/10.1051/0004-6361/201220697.
[49] M. Alford, A. Sedrakian, Compact stars with sequential QCD phase transitions, Phys. Rev. Lett. 119 (2017) 161104, https://doi.org/10.1103/PhysRevLett.119.161104.
[50] G. Raaijmakers, T.E. Riley, A.L. Watts, A pitfall of piecewise-polytropic equation of state inference, Mon. Not. R. Astron. Soc. 478 (2018) 2177–2192, https://doi.org/10.1093/mnras/sty1052.
[51] J.-E. Christian, J. Schaffner-Bielich, Twin stars and the stiffness of the nuclear equation of state: ruling out strong phase transitions below $1.7n_0$ with the new NICER radius measurements, Astrophys. J. Lett. 894 (2020) L8, https://doi.org/10.3847/2041-8213/ab8af4.
[52] J.P. Pereira, M. Bejger, N. Andersson, F. Gittins, Tidal deformations of hybrid stars with sharp phase transitions and elastic crusts, Astrophys. J. 895 (2020) 28, https://doi.org/10.3847/1538-4357/ab8aca.
[53] M. Ferreira, R.C. Pereira, C. Providência, Neutron stars with large quark cores, Phys. Rev. D 101 (2020) 123030, https://doi.org/10.1103/PhysRevD.101.123030.
[54] D. Blaschke, A. Ayriyan, D.E. Alvarez-Castillo, H. Grigorian, Was GW170817 a canonical neutron star merger? Bayesian analysis with a third family of compact stars, Universe 6 (2020) 81, https://doi.org/10.3390/universe6060081.
[55] A. Bauswein, S. Blacker, V. Vijayan, N. Stergioulas, K. Chatziioannou, et al., Equation of state constraints from the threshold binary mass for prompt collapse of neutron star mergers, arXiv:2004.00846, 2020.
[56] H. Tan, J. Noronha-Hostler, N. Yunes, Kinky neutron stars in light of GW190814, arXiv:2006.16296, 2020.
[57] V. Dexheimer, R.O. Gomes, T. Klahn, S. Han, M. Salinas, GW190814 as a massive rapidly-rotating neutron star with exotic degrees of freedom, arXiv:2007.08493, 2020.
[58] N.K. Glendenning, Neutron stars are giant hypernuclei?, Astrophys. J. 293 (1985) 470–493, https://doi.org/10.1086/163253.
[59] N.K. Glendenning, S.A. Moszkowski, Reconciliation of neutron-star masses and binding of the Λ in hypernuclei, Phys. Rev. Lett. 67 (1991) 2414–2417, https://doi.org/10.1103/PhysRevLett.67.2414.
[60] I. Vidaña, A. Polls, A. Ramos, H.-J. Schulze, Hypernuclear structure with the new Nijmegen potentials, Phys. Rev. C 64 (2001) 044301, https://doi.org/10.1103/PhysRevC.64.044301.
[61] L. Tolos, M. Centelles, A. Ramos, Equation of state for nucleonic and hyperonic neutron stars with mass and radius constraints, Astrophys. J. 834 (2017) 3, https://doi.org/10.3847/1538-4357/834/1/3.
[62] J.J. Li, W.H. Long, A. Sedrakian, Hypernuclear stars from relativistic Hartree-Fock density functional theory, Eur. Phys. J. A 54 (2018) 133, https://doi.org/10.1140/epja/i2018-12566-6.
[63] J.J. Li, A. Sedrakian, Constraining compact star properties with nuclear saturation parameters, Phys. Rev. C 100 (2019) 015809, https://doi.org/10.1103/PhysRevC.100.015809.
[64] D. Vretenar, A.V. Afanasjev, G.A. Lalazissis, P. Ring, Relativistic Hartree–Bogoliubov theory: static and dynamic aspects of exotic nuclear structure, Phys. Rep. 409 (2005) 101–259, https://doi.org/10.1016/j.physrep.2004.10.001.
[65] J. Meng, H. Toki, S.-G. Zhou, S.Q. Zhang, W.H. Long, L.S. Geng, Relativistic continuum Hartree Bogoliubov theory for ground-state properties of exotic nuclei, Prog. Part. Nucl. Phys. 57 (2006) 470–563, https://doi.org/10.1016/j.ppnp.2005.06.001.
[66] G.A. Lalazissis, T. Nikšić, D. Vretenar, P. Ring, New relativistic mean-field interaction with density-dependent meson-nucleon couplings, Phys. Rev. C 71 (2005) 024312, https://doi.org/10.1103/PhysRevC.71.024312.
[67] V. Pascalutsa, M. Vanderhaeghen, S.N. Yang, Electromagnetic excitation of the $\Delta(1232)$-resonance, Phys. Rep. 437 (2007) 125–232, https://doi.org/10.1016/j.physrep.2006.09.006.
[68] X. Roca-Maza, X. Viñas, M. Centelles, P. Ring, P. Schuck, Relativistic mean-field interaction with density-dependent meson-nucleon vertices based on microscopical calculations, Phys. Rev. C 84 (2011) 054309, https://doi.org/10.1103/PhysRevC.84.054309.
[69] M. Oertel, M. Hempel, T. Klähn, S. Typel, Equations of state for supernovae and compact stars, Rev. Mod. Phys. 89 (2017) 015007, https://doi.org/10.1103/RevModPhys.89.015007.
[70] M. Dutra, O. Lourenço, J.S. Sá Martins, A. Delfino, J.R. Stone, et al., Skyrme interaction and nuclear matter constraints, Phys. Rev. C 85 (2012) 035201, https://doi.org/10.1103/PhysRevC.85.035201.
[71] M. Dutra, O. Lourenço, S.S. Avancini, B.V. Carlson, A. Delfino, et al., Relativistic mean-field hadronic models under nuclear matter constraints, Phys. Rev. C 90 (2014) 055203, https://doi.org/10.1103/PhysRevC.90.055203.
[72] H. Tong, X.-L. Ren, P. Ring, S.-H. Shen, S.-B. Wang, J. Meng, Relativistic Brueckner-Hartree-Fock theory in nuclear matter without the average momentum approximation, Phys. Rev. C 98 (2018) 054302, https://doi.org/10.1103/PhysRevC.98.054302.
[73] J. Antoniadis, P.C.C. Freire, N. Wex, T.M. Tauris, R.S. Lynch, et al., A massive pulsar in a compact relativistic binary, Science 340 (2013) 1233232, https://doi.org/10.1126/science.1233232.
[74] M.W. Coughlin, T. Dietrich, Z. Doctor, D. Kasen, S. Coughlin, et al., Constraints on the neutron star equation of state from AT2017gfo using radiative transfer

simulations, Mon. Not. R. Astron. Soc. 480 (2018) 3871, https://doi.org/10.1093/mnras/sty2174.
[75] K. Kiuchi, K. Kyutoku, M. Shibata, K. Taniguchi, Revisiting the lower bound on tidal deformability derived by AT2017gfo, Astrophys. J. Lett. 876 (2019) L31, https://doi.org/10.3847/2041-8213/ab1e45.
[76] B.P. Abbott, R. Abbott, T.D. Abbott, S. Abraham, F. Acernese, et al., GW190425: observation of a compact binary coalescence with total mass $\sim 3.4\,M_{\odot}$, Astrophys. J. Lett. 892 (2020) L3, https://doi.org/10.3847/2041-8213/ab75f5.
[77] P. Danielewicz, R. Lacey, W.G. Lynch, Determination of the equation of state of dense matter, Science 298 (2002) 1592–1596, https://doi.org/10.1126/science.1078070.
[78] T. Nozawa, N. Stergioulas, E. Gourgoulhon, Y. Eriguchi, Construction of highly accurate models of rotating neutron stars - comparison of three different numerical schemes, Astron. Astrophys. Suppl. Ser. 132 (1998) 431–454, https://doi.org/10.1051/aas:1998304.
[79] W.M. Spinella, F. Weber, Dense baryonic matter in the cores of neutron stars, in: Topics on Strong Gravity, World Scientific, 2020, pp. 85–152.
[80] G. Malfatti, M.G. Orsaria, I.F. Ranea-Sandoval, G.A. Contrera, F. Weber, Delta baryons and diquark formation in the cores of neutron stars, arXiv:2008.06459, 2020.
[81] T. Schürhoff, S. Schramm, V. Dexheimer, Neutron stars with small radii - the role of Δ resonances, Astrophys. J. 724 (2010) L74, https://doi.org/10.1088/2041-8205/724/1/L74.
[82] A. Taninah, S. Agbemava, A. Afanasjev, P. Ring, Parametric correlations in energy density functionals, Phys. Lett. B 800 (2020) 135065, https://doi.org/10.1016/j.physletb.2019.135065.